

## Analysis of DSC results by integration

Joseph H. Flynn

*Scientific Thermal Research and Data Analysis (STRDA), 5309 Iroquois Road, Bethesda, MD 20816 (USA)*

(Received 27 July 1992)

### Abstract

The integration of data from differential scanning calorimetry to obtain enthalpy vs. time or temperature curves can be performed easily and painlessly with modern thermoanalytical instruments interfaced with computers. This paper reviews old techniques and develops new ones for determining proper thermodynamic quantities and temperatures, and degrees of conversion from the integrated curves.

Methods for using the isothermal baseline rather than the transient one for minimizing the displacement from it during a constant heating rate experiment and for calibrating the isothermal temperature are described. Integration avoids errors due to kinetics effects and changes in interfacial resistance in the determination of heat capacity. The thermodynamic or "fictive" glass transition temperature and change in specific heat at the glass transition are determined more easily and in a correct manner by the integration method. The analysis of both sharp and diffuse first order transitions are discussed. Thermodynamically correct temperatures and heats of transition and reaction are obtained through integration. Application of the lever rule to isothermal "tie lines" is used to obtain the correct "fraction reacted" during transitions, and methods for compensating for weight loss and heat of evaporation are discussed. Purity determination by the stepwise isothermal method is briefly reviewed.

### INTRODUCTION

The concept of integrating differential scanning calorimetry (DSC) curves, i.e. determining changes in enthalpy from the integration of heat capacity at constant pressure data, is hardly a recent innovation. Ever since the ice calorimeter was developed by Lavoisier and Laplace in 1783 [1], scientists have, in one way or another, been obtaining "heats" from experimental "heat capacities". It is surprising, therefore, that thermal analysts do not automatically display their integrated DSC data because the interpretation of these "enthalpic" results is often much more obvious and straightforward, and one can often avoid many problems and pitfalls encountered during the interpretation of the derivative DSC traces.

Now that most thermoanalytical experimental results are obtained through a computer interface and mathematical manipulation of these data is routine, there is no excuse for not taking advantage of this simplifying treatment during the design and analysis of DSC experiments.

This paper discusses ways of obtaining the correct baseline for integration of a DSC curve, calibrating temperature, measuring heat capacity, glass transition temperatures and  $C_p$  changes, determining purity from the van't Hoff equation, determining transition temperature and enthalpy for sharp and diffuse first order transitions, determining degree of conversion by applying the lever rule to integral curves, and ways for compensating for weight loss and latent heat effects during first order transitions.

#### BASELINE DETERMINATION

In order to integrate a DSC curve (i.e. the rate of heat change (power) as a function of temperature or time) and thus to determine heats of transition etc., it is necessary to establish a baseline to bound the area which is to be integrated. In the absence of any physical or chemical transformation, the isothermal baseline reaches a steady value after a very short instrumental warm up period, during which any transient effects decay. This steady value depends only on the difference in heat flows through the sample and reference calorimeters or platforms at that temperature. A series of steady state values at successively higher or lower isothermal temperatures obviously delineate this stable baseline and, unlike the so-called baseline obtained at constant heating rate, it is unaffected by transient effects such as changing patterns of heat flow and contact at solid–solid interfaces and inherent kinetic lags, which occur when a system is being heated or cooled. Further, in the case of a first order transition, obtaining an “isothermal” baseline by the linear extrapolation of the isothermal baseline from before the transition is justifiable and can be tested in some cases by pauses at various temperatures within the temperature range of the transition. In any event, any deviation in its linearity can be assessed from a “blank” experiment (with empty pans).

If the heat capacity difference between the sample and reference sides of the DSC is large, then there will be a large displacement of the DSC trace when the system is heated or cooled at a constant rate. This displacement will be proportional to the heat capacity difference between the two sides multiplied by the rate of temperature change. When such a large displacement occurs, the imprecision in measuring small heat changes by integration of heat capacity data increases considerably. However, such large displacements can be removed quite simply. Any large disparity between the heat capacities of the reference and sample sides of a DSC can be compensated for by adding (usually to the reference side of the DSC) the proper amount of thermally inert material, e.g. (pieces of) aluminum sample pan lids. This procedure diminishes the area to be integrated and thus increases the sensitivity of the integrated curve to the heat changes.

When the temperature of the DSC is changed, the DSC trace at constant heating rate will show some curvature, even in the absence of an enthalpic

event, due to the difference in emissivities of the sample and reference sides. This difference and resulting curvature may increase as the instrument ages. The emissivities can be more closely matched by applying an area of dark coating to one side of the DSC [2]. However, the method used to straighten the baseline in modern instruments is to ramp a little extra current to one of the sides. This is reasonably successful in straightening this “dynamic base line” but results in a difference between the temperatures of the sample and reference sides of the calorimeter which may be as large as several degrees [3].

As a result of all of the above and many other complications, the “isothermal” baseline, rather than the “dynamic” baseline, is used in this paper as a boundary for the area to be integrated. The establishment of an isothermal baseline is described in the isothermal temperature calibration which follows.

#### ISOTHERMAL TEMPERATURE CALIBRATION

One should integrate a DSC trace between two isothermal temperatures, so it is important that these isothermal temperatures be calibrated with high precision. The isothermal temperature may be calibrated from transition temperatures such as the melting point of indium or from sharp reproducible transitions of other materials [4]. An example of this technique is shown in Fig. 1. Here the programmed temperature was raised in 0.1 K increments from 427.8 to 428.5 K. The baseline along the abscissa

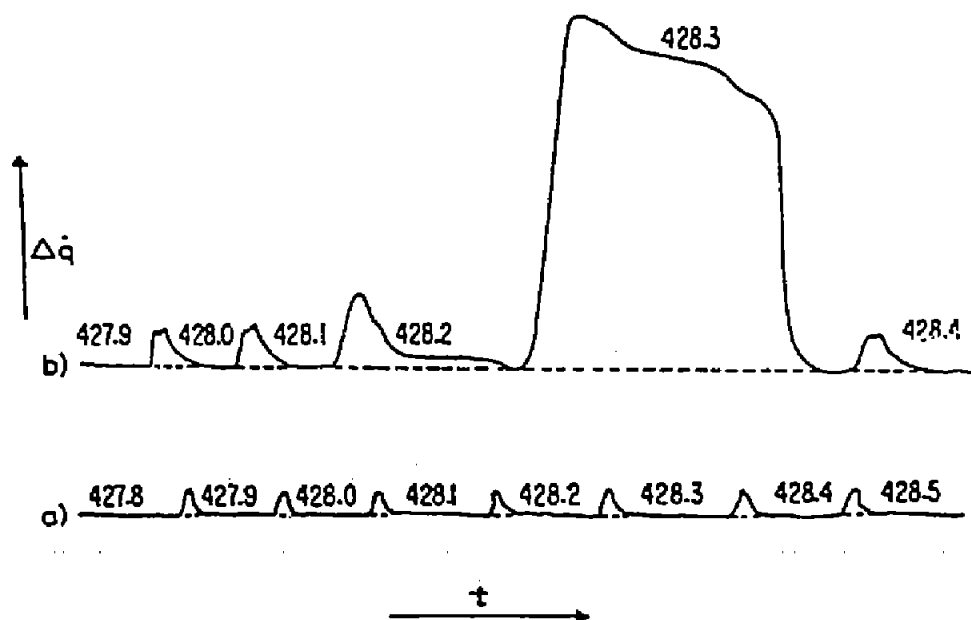


Fig. 1. A DSC trace (power difference vs. time) showing successive isothermal steps: (a) empty pans; (b) 8.00 mg of 99.99% indium in the sample pan. The numbers are the programmed temperatures in kelvin. The temperature was increased by 0.1 K at the beginning of each deflection.

(drawn through the isothermal pauses) is by definition the isothermal baseline which was discussed in the previous section. (Obviously, this isothermal baseline can be extended over a much broader temperature range.)

The areas between the displacements and the baseline in Fig. 1, curve (a) (for empty sample pans), when the programmed temperature is increased by 0.1 K increments, are proportional to the enthalpy change, i.e. the integral of the differences in heat capacity between the sample and reference sides over the 0.1 K temperature step. (Actual integration is unnecessary here because we are only interested in identifying the temperatures, not the magnitude of the enthalpy changes.) The large displacements in Fig. 1, curve (b) result from the increased heat capacity of the sample side due to the presence of an 8.00 mg specimen of 99.99% indium. The increase in the area of the displacement at the programmed temperature increment of 428.1–428.2 K is due to the van't Hoff "impurity tail" of the indium melting transition and/or a slight "overshoot" during the temperature increase. The very large area produced by the temperature change 428.2–428.3 K identifies this programmed temperature range with the melting point of the indium.

In order to calculate the change in enthalpy over a temperature range, one must integrate the area between the isothermal baseline and the DSC curve for the sample of interest and then subtract from this enthalpy the enthalpy obtained from a similar integration between the DSC curve and isothermal baseline for the same temperature range for a run made with an empty sample pan. That is, in Fig. 1 one must subtract the areas of the "empty pan" curve (a) from the areas of curve (b). If one has compensated for the heat capacity difference between the sample and reference sides, the areas of curve (a) will be very small for short temperature or time ranges. No enthalpic events occur during the empty pan run (curve (a)) so the area can be determined for much larger temperature jumps, say of 20 or 30 degrees, and an average area per degree calculated. Then the appropriate average area (in the above case, for one tenth of a degree) subtracted from each of the one tenth degree jumps areas of Fig. 1, curve (b). As previously stated, the integration of the areas is unnecessary for isothermal temperature calibration, but integration is required for a case involving a quite similar experimental procedure (stepwise impurity determination) described later in this paper.

#### DETERMINATION OF HEAT CAPACITY

The well-known way of measuring specific heat capacity by DSC [5] is illustrated in Fig. 2. An empty sample pan is heated or cooled at a constant rate of temperature change between two isothermal temperatures  $T_1$  and  $T_2$ . This is repeated, first with a material of known  $C_p$  (e.g. alumina) in the sample pan and then with the specimen of interest. The specific heat

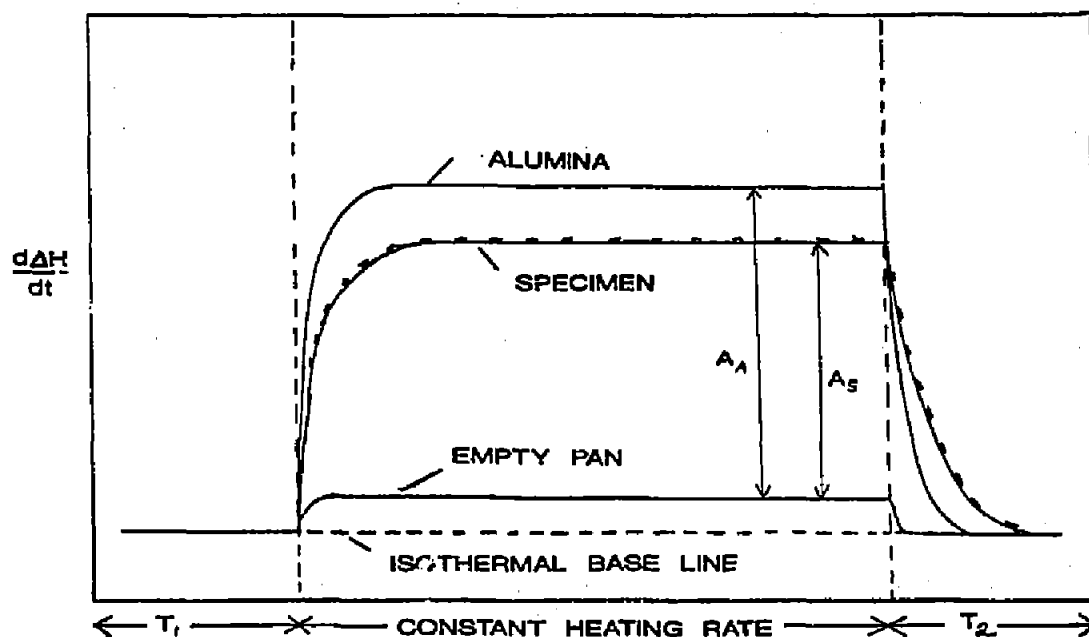


Fig. 2. The dynamic method for specific heat capacity determination by DSC: power vs. temperature.

capacity of the sample  $C_p(\text{sample})$  at any temperature in the range is calculated from the known value of  $C_p(\text{alumina})$  from the equation

$$C_p(\text{sample}) = C_p(\text{alumina}) \times [wt(\text{alumina})/wt(\text{sample})] \times [A(\text{sample})/A(\text{alumina})] \quad (1)$$

where  $wt$  is weight and  $A$  is amplitude, i.e. the distance along the ordinate between the alumina or sample curve and the empty pan curve at the chosen temperature. The accuracy of heat capacity measurement by this method is usually about  $\pm 5\%$  which can be reduced to about 1% by meticulous experimental procedure [6, 7]. There are several causes for this lack of precision. One serious problem is that of maintaining a constant thermal resistance across solid–solid interfaces. In this case, these interfaces are between the calorimeter or platform and the sample pan and between the sample pan and the alumina or specimen. Any movement resulting from purge gas flow, vibration, specimen buckling, sintering or melting, or (most importantly) from removing and replacing alumina and sample specimens, will affect these thermal resistances and alter the heat flow pattern of the system. Differences between the thermal conductivity of the specimen and the calibrating material will also introduce error into the calculation.

The thermal resistance between the pan and the calorimeter can be reduced to about one third of its value and rendered more reproducible by putting into the pan–calorimeter interface a drop of “thermal lubricant” e.g. high viscosity silicone oil (for temperatures below 200°C) [8]. In any event, in a constant rate of temperature change experiment such as this,

there is an inherent lag in the amplitude when the heat capacity is changing with temperature. (The decrease in area (and amplitude) resulting from this lag is not regained until a new isothermal temperature is established.) This can amount to several percent error in heat capacity measurement for poorly conducting specimens [9].

However, all of the problems inherent in the above dynamic method can be avoided by the integration method, i.e. using the DSC as a calorimeter [4]. In a traditional calorimeter, a metered amount of power is added to the system and the compensating temperature change is measured. To use the DSC as a calorimeter, a metered temperature change can be introduced and then the power that the DSC heaters add to the system to compensate for this temperature change is measured. As before, the DSC is operated between two isothermal temperatures  $T_1$  and  $T_2$ . (In this case, rate of temperature change is immaterial; thus, we will use the curves in Fig. 2 to illustrate this method.) As before, experiments are performed first with the empty sample pan and then with the sample of interest. The two curves are then integrated between their isothermal baselines and their displacements during the temperature change. If the enthalpic calibration constant  $K$  for the DSC has been accurately measured, then the enthalpy change,  $\Delta H$ , may be determined from the integrated areas and therefore the average specific heat capacity for the unknown sample over the temperature range  $T_1$ – $T_2$ , will be given by eqn. (2).

$$\begin{aligned} C_p(T_1, T_2) &= K[AREA(\text{sample}) - AREA(\text{empty})]/(T_2 - T_1) \\ &= [\Delta H(\text{sample}) - \Delta H(\text{empty})]/(T_2 - T_1) \end{aligned} \quad (2)$$

In heat capacity determination there is no special advantage in the analysis of the data to be gained by displaying the integrated enthalpy vs. temperature plot.

The main source of error in eqn. (2) is the calculation of the enthalpic constant for the instrument, which is obtained by using alumina or some other standard for which the heat capacity has been accurately determined. As in all calorimetric studies, an average value for the function  $C_p$  over a temperature interval is obtained. This temperature interval can be shortened or, better yet, experiments with overlapping intervals may be performed as needed to extend and to bring out the detail of the  $C_p$  vs. temperature curve for the substance. The total enthalpy change between two isothermal temperatures is used for these calculations, so the precision is much greater than that obtained from the conventional measurement of  $C_p$  from the amplitude of the derivative curve as illustrated in Fig. 2.

#### DETERMINATION OF THE GLASS TRANSITION TEMPERATURE

The glass transition temperature  $T_g$  seems simple enough when it is defined thermodynamically as the point on an enthalpy (or volume) vs. temperature graph at which the (supercooled) liquid and the glass curves

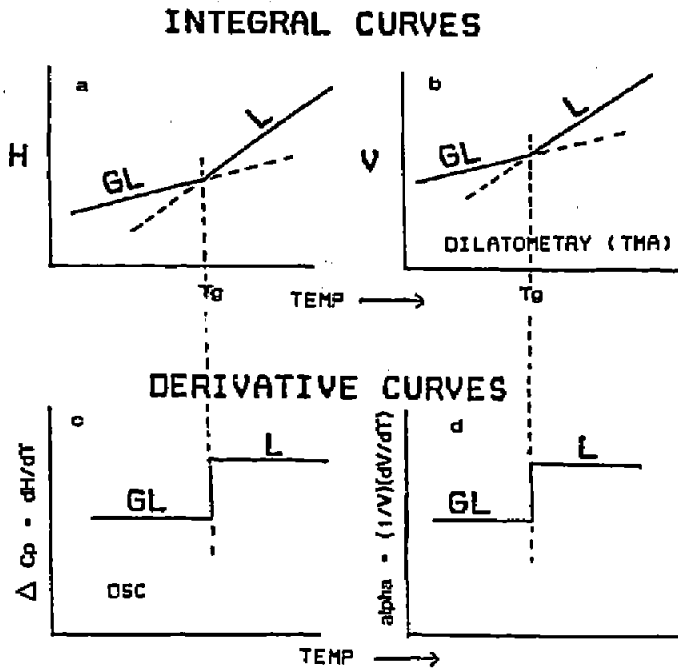


Fig. 3. The glass transition temperature ("ideal" second order transition curves): (a) enthalpy vs. temperature; (b) volume vs. temperature; (c) heat capacity vs. temperature; (d) coefficient of expansion vs. temperature.

intersect (as shown in the "ideal case" schematic in Fig. 3). Indeed, this is the way that it is determined from a thermomechanical analysis (TMA) plot of volume (or a dimension) change vs. temperature where an extrapolation is made to the intersection of the two curves as shown in Fig. 3(b). However, the traditional technique for determination of  $T_g$  by DSC is to define it at the discontinuity of the derivative curve (step function), as shown in Fig. 3(c). The integration of the DSC curve (as in Fig. 3(a)) to obtain the thermodynamic (or fictive)  $T_g$  was suggested many years ago by Flynn [4] and Richardson and Savill [10]; only in the last few years have computer routines been developed to perform this relatively simple operation [11].

The problems involved in using the derivative DSC curve to obtain the glass transition temperature are manifold. Two innate complications in glass transition measurement are illustrated schematically in Fig. 4. First, the glass transition is kinetically sluggish, so it takes place over a temperature range which may be quite large at conventional heating rates. This causes the glass transition obtained from DSC to be a sigmoidal curve rather than a step function, as is illustrated schematically in Fig. 4(a). Secondly, the glassy state is imperfect and cannot be well defined. Therefore, if one cools a material rapidly from the liquid state (quenches it), this liquid is frozen into a low density glass with a high enthalpy (as illustrated schematically by GL(1) in Fig. 4(b)). However, if the material is

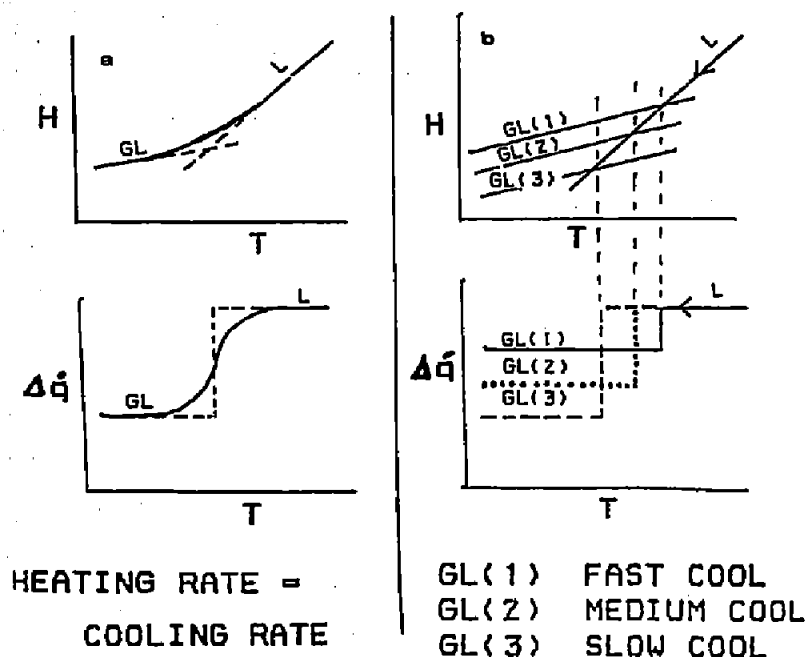


Fig. 4. The glass transition temperature—two complications: (a) kinetics structure; (b) multiple glassy states: enthalpy vs. temperature and heat capacity vs. temperature curves: GL(1), low density glass; GL(2), intermediate density glass; GL(3), high density glass.

cooled slowly (i.e. it is allowed to anneal) the molecules relax into a high density glassy state of lower enthalpy (as illustrated by GL(3) in Fig. 4(b)). There is, of course, an almost continuous spectrum of intermediate glassy states (e.g. GL(2) in Fig. 4(b)) which have intermediate densities and enthalpies.

We discuss from a phenomenological perspective two examples of what may occur when a glass is heated through its  $T_g$  in DSC [4]. These two cases are shown in Fig. 5. In Fig. 5, case (I), a liquid is cooled slowly into a high density low enthalpy glassy state and then heated rapidly. In effect, the heating glass “overshoots” the liquid curve because its “relaxation time” in this lower temperature range is long in comparison to the rate of heating. As the temperature increases, the relaxation time for the glass to liquid process decreases and the system “catches up” to the liquid curve and, as a result, one sees what appears to be an endothermic first order peak at the end of the glass transition [4, 12]. This happens often during the measurement of the  $T_g$  of amorphous polymeric materials. This peak is illustrated by curve (I) in the lower DSC plot in Fig. 5. In case (II), the substance is rapidly quenched into a low density “imperfect” glass, as in Fig. 5. It is then heated slowly through the glass transition temperature region. As the glass transition temperature is approached, the glass begins to “perfect” itself, i.e. slowly anneal itself into a lower enthalpy glassy state.



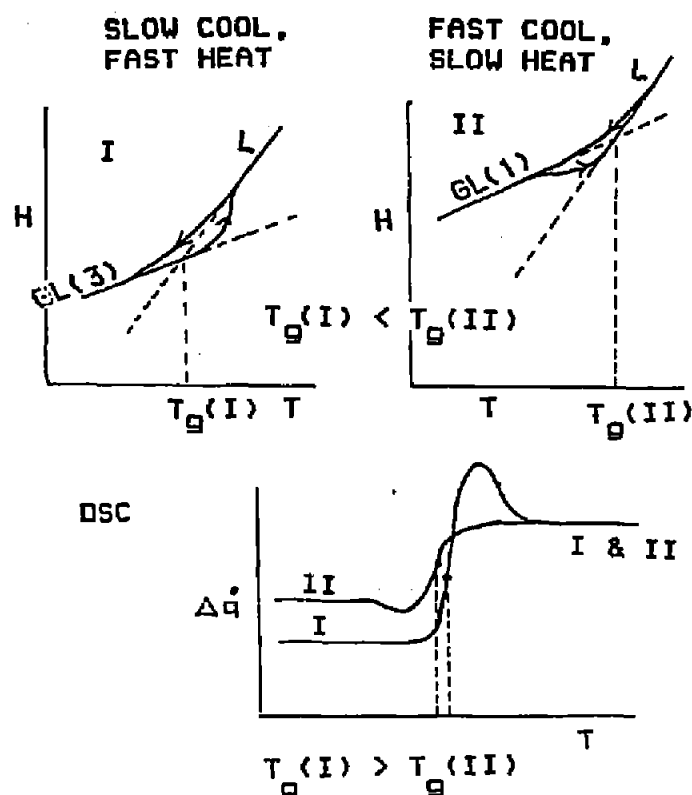


Fig. 5. The effect of cooling rate on glass transition temperature determination by DSC: (I) enthalpy vs. temperature, slow cooling and fast heating; (II) enthalpy vs. temperature, fast cooling and slow heating; DSC curves for cases (I) and (II).

This occurs until the supercooled liquid curve is neared and the transition from the glass to the liquid phase begins to take place at a more rapid pace than the annealing process. This annealing process may produce what appears to be a small exothermic peak at the beginning of the glass transition. This peak is illustrated by curve (II) in the lower DSC plot in Fig. 5.

It can be seen from the enthalpy vs. temperature curves in Fig. 5 that the correct glass transition temperature (obtained from the extrapolated intersection of the glass and liquid curves) is lower for the high density glass GL(3) in Fig. 5(I) than for the low density glass GL(1) in Fig. 5(II). This is to be expected. However, if the customary method of determining the glass transition temperature from the derivative DSC curves of Fig. 5 is used (i.e. taking the temperature at which the DSC trace has reached the midpoint of the amplitude of  $\Delta C_p$  between the "before" and "after" curves) then incorrect values for the  $T_g$  values are obtained, e.g. the annealed glass GL(3) appears to have a higher glass transition temperature than the quenched glass GL(1).

Many other complicating phenomena can occur in the glass transition

region. As the glass is heated through its transition, the atoms and molecules are released from their rigid structure and are able to do what they were unable to do before because of their immobile condition. Strains introduced during cooling or mechanical working are released, causing exothermic displacements. Occluded gases or vapors start to escape, causing another enthalpic displacement. Some thermosetting polymers may have an “annealing peak” in the middle of the glass transition. If the specimen was previously quenched, then cold recrystallization can occur with a release of enthalpy. Chemical reactions may suddenly flare up at a greatly increased rate owing to the increased mobility of the reactants. These reactions may consist of either synthesis, (e.g. further cure of a resin) or a decomposition reaction. These reactions may be either endothermic or exothermic. An additional problem is that, owing to the sluggishness of the glass transition, the region of heat capacity change for some materials may stretch over a range of several tens of degrees of temperature and, in the case of highly cross-linked polymers for example, the change in heat capacity in the DSC curve (or change in slope of enthalpy curve) in the glass transition region will be very slight. As a result, the DSC trace in the glass transition region may include considerable collateral enthalpic structure which can make  $T_g$  determination difficult (if not impossible) in some cases.

Some “typical” DSC glass transition curves are shown in Fig. 6. These types of derivative curves are most difficult to interpret. However, by using the integral curves of enthalpy vs. temperature, the slopes of the liquid and glassy curves can often be extrapolated to their intersection at  $T_g$  from regions beyond those where the complicating effects occur. Further, for the

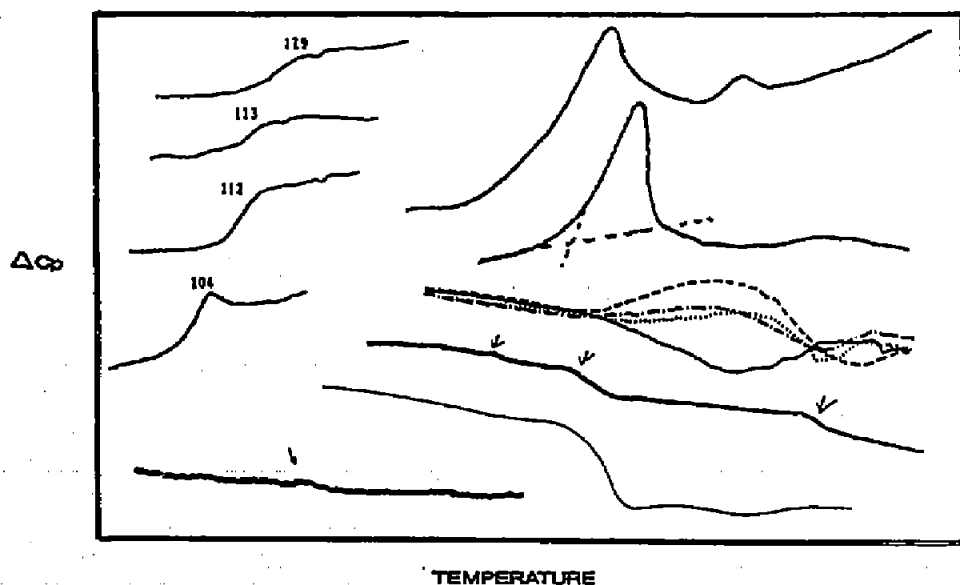


Fig. 6. Some DSC curves for glass transitions which are difficult to interpret. (Published DSC glass transition curves tend to be the “cream of the crop”. Most of the really ugly curves are undoubtedly filed away and never seen in print.)

integrated curves the differences in slopes between the extended glass and liquid curves permit a better calculation of the  $\Delta C_p$  at the glass transition.

#### FIRST ORDER TRANSITION MEASUREMENT

First order transitions may be divided into two types. The first is a sharp transition such as the melting or freezing of a pure low molecular weight material of high thermal conductivity. For a sharp first order transition, measured by DSC at constant heating rate, the temperature increment during which the heat must flow between the DSC heater and the specimen in order to match its heat of transition is larger than the temperature range of the transition. In this case, the rate of measurement of the transition by DSC is heat flow limited. At constant heating rate, the leading edge of this endo or exothermic peak should be linear and its slope equal to the heating rate divided by the thermal resistance between the heater and the specimen. The second type of first order transition is a diffuse transition. In this case the shape of the DSC peak is limited by the kinetics of the transition. Examples of diffuse transitions are those of the melting of many polymers and those of chemical reactions. We discuss the interpretation and measurement of heats and fractional conversions for both of these types of transitions.

However, before discussing the integration of first order transition peaks it is well to point out a basic misconception by many thermal analysts which flaws their analysis of first order transitions obtained from DSC data. Thermodynamic quantities such as enthalpy, entropy, free energy, volume, etc. are defined at a specified temperature, pressure, chemical composition, etc. However, because scientists in the field of thermal analysis are dealing with measurements at continually changing temperatures, they have developed the misconceived practice of measuring heats (which they often mistakenly call enthalpies) of transitions and reactions over a temperature range rather than at a specific temperature.

There might be an argument for defining the heat of transition or reaction obtained from the area under a DSC peak as the heat (at constant heating rate) for the temperature range  $T_1$ – $T_2$ , the temperatures at the beginning and end of the DSC peak. However, one does not define any other property which changes with temperature (such as volume) over a temperature range and most scientists would not find this an acceptable practice.

In the determination of the heat of transition from the area of a DSC peak, there is no problem in bounding it by the linear extrapolations of the dynamic baselines, before and after the DSC transition, when these extrapolations meet to form a straight line, i.e. when there is insignificant change in heat capacity during the transition. However, for the case where

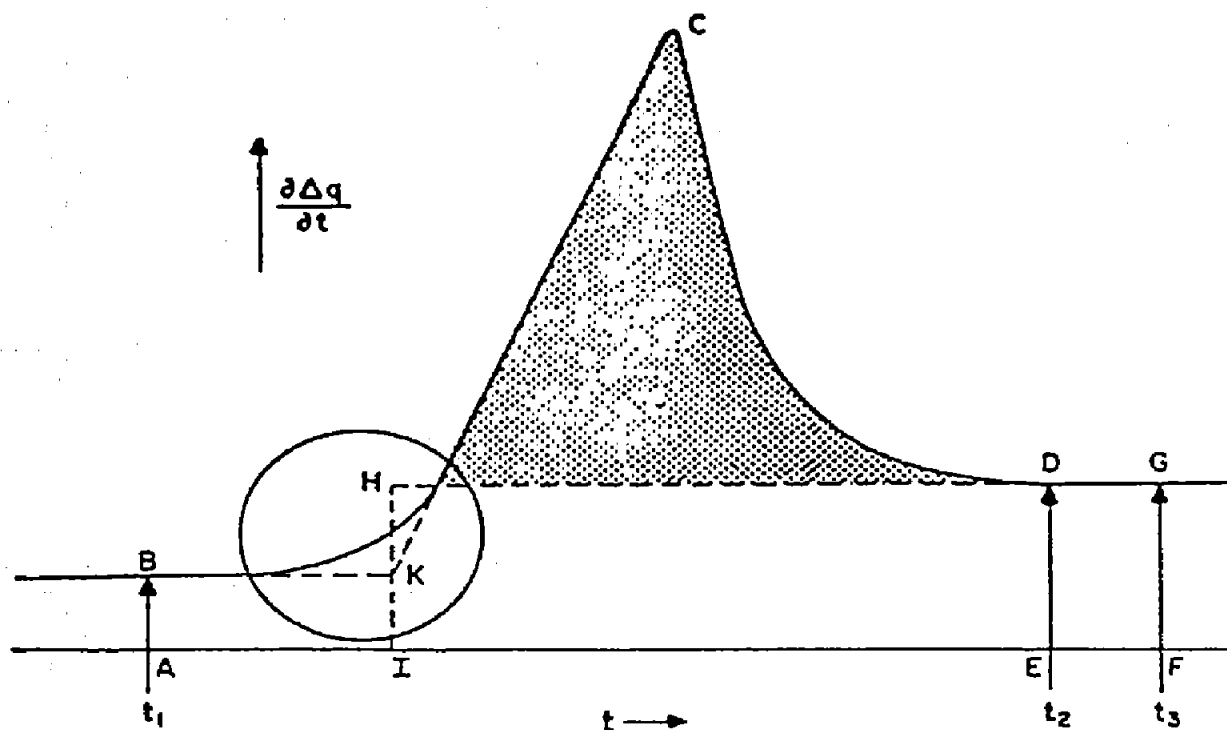


Fig. 7. Drawing the correct base line on a DSC thermogram for a heat of transition [14].

there is a significant heat capacity change, Adam and Muller (for DTA) [13] and Guttman and Flynn (for DSC) [14] demonstrated that the enthalpy of transitions can be correctly obtained by constructing a step function between the extrapolations of the “before” and “after” baselines to a selected temperature at which the enthalpy is to be calculated. (There is still a slight kinetics correction for thermal lags when using this step function for the baseline to calculate enthalpy [9].) This case is illustrated in Fig. 7. Here, for a sharp transition, the transition temperature at which the enthalpy was calculated was chosen to be the “onset” temperature. Once the enthalpy is calculated at any one temperature, it may be calculated at another temperature by applying Kirchoff’s equation [15] for the change in heat capacity integral. (Recently, over twenty years after the publication of refs. 13 and 14, several DSC instrument manufacturers have finally developed routines for calculating such a baseline.) However, we shall see that prior integration of the DSC peak simplifies these calculations and clears up most of the ambiguities in the selection of proper “before” and “after” dynamic baselines.

Integration of first order transition peaks is always performed whenever enthalpies or heats of transition or reaction are determined from them. However, the integrated enthalpy vs. temperature (or time) curves are seldom displayed or included in a publication. Before we describe the interpretation of an integrated first order DSC peak, there is another rather obvious factor that is often overlooked. Not only must one define the

transition or reaction temperature, but one also must define the stoichiometric equation for the transition (or reaction) itself. This is not an important factor for systems involving simple condensed phase transitions, e.g. Solid A  $\rightarrow$  Solid B, or Solid B  $\rightarrow$  Liquid. In more complex systems such as chemical reactions, especially where a change in mass is involved, such stoichiometric equations are essential both for defining the enthalpy and determining the fractional conversion. We illustrate the importance of these considerations later by presenting as an example the measurement of the chemical cure (polymerization) of a resin as measured from its heat of reaction by a DSC. Such a system includes many of the factors which complicate the analysis of these DSC traces.

However, we first illustrate the integration of a simple case in which the above complicating factors are not present. In Fig. 8 (top) we see a schematic DSC trace of an endothermic first order transition during which there is a change in the heat capacity of the specimen, i.e. the extrapolated dynamic "baselines" before and after the transition do not intersect to form a straight line.

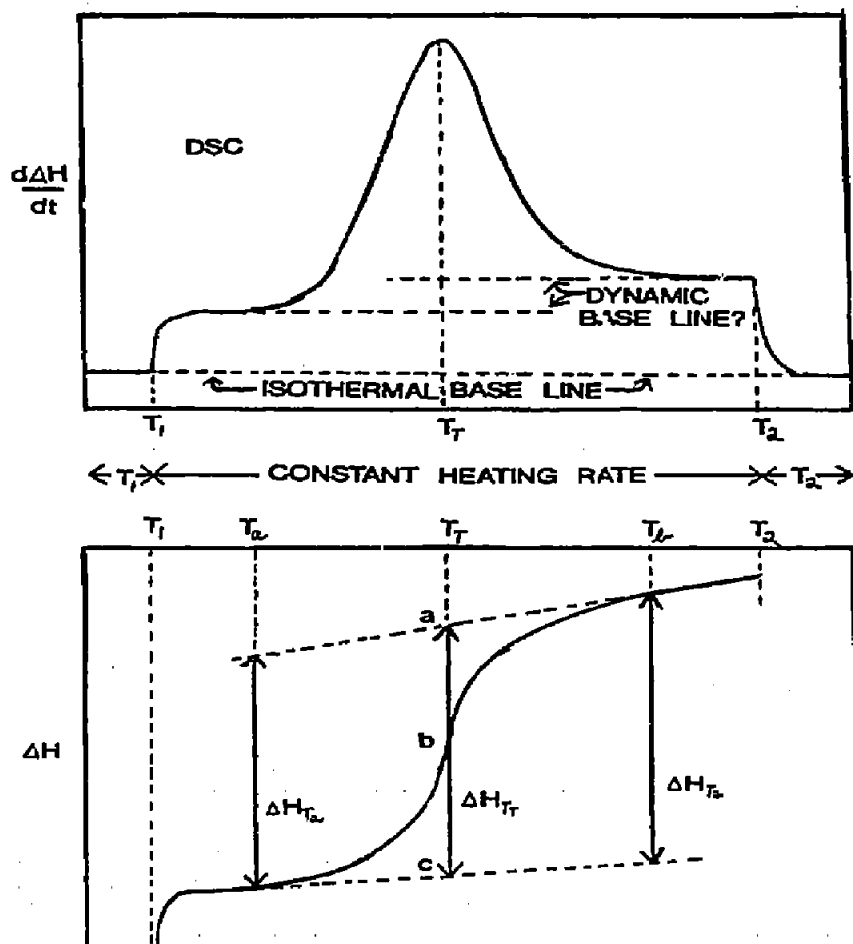


Fig. 8. Integration of a first order transition during which there is a heat capacity (baseline) change: schematic of DSC trace and the integrated  $\Delta H$  vs. temperature curve.

It is obvious that the proper enthalpy of transition can be obtained at a temperature ( $T_T$ ) by using the step function baseline as suggested above. However, it must be calculated separately at each different temperature. Further, the measurement of the fraction reacted  $\alpha$  at  $T_T$ , say, from the fractional area divided by the total area is ambiguous and unobtainable. (An incorrect fraction reacted is obtained by bounding the area with a straight line baseline connecting the “before” and “after” dynamic baselines.) In 1969 Brennan et al. [16] developed an iterative method for determining the baseline in cases where the heat capacity change is due to the immediate loss of a volatile product. This method results in a sigmoidal baseline and has recently been included in the software of several commercial instruments.

If the area between the DSC curve and its isothermal baseline is integrated, we obtain the  $\Delta H$  vs.  $T$  plot shown in Fig. 8 (bottom). The simplicity of determining enthalpies and fractions reacted from the integral curve is immediately apparent. The reaction enthalpy is obtained from the vertical distance (ac) between the extrapolated “before” and “after” enthalpy curves at any desired temperature (e.g.  $T_a, T_T, T_b$ ) and the Kirchhoff correction is automatically taken care of by the differing slopes of the “before” and “after” enthalpy curves. Most importantly, the fraction reacted (fractional conversion) is correctly and simply obtained from application of the “lever rule” to the distances along the vertical “tie lines” at any temperature. For example, the fractional conversion at  $T_T$  is  $bc/ac$ .

The next example we discuss is the exothermic cure of a resin to form a polymeric material. These reactions can include most of the complicating factors which can occur in a DSC measurement of a first order transition involving an endothermic or exothermic chemical reaction.

There are many factors involved in the cure of a resin which complicate the interpretation of its DSC trace. The first is a very fundamental one. We know from the curves of systems of homologous monomers such as acrylates that the magnitude of the enthalpy of cure depends upon steric strains or hindrances in the structure of the particular monomer. That is, monomers with more strained structures have lower enthalpies of cure than those without such strains. As a thermosetting resin such as an epoxy cures, it is obvious that similar strains are produced by the crosslinking process, so not only is the rate of cure affected, but the enthalpy of cure may also decrease as the cure proceeds and the structures of the reactants become more complex. (This change in reaction enthalpy due to changes in steric strains must also occur in many inorganic systems.) In the calculation of conversion from fractional areas or tie lines, the fractional conversion values should be weighted by the continually changing enthalpy of cure. However, no way of taking this factor into account is known by this author.

The second factor is that mass loss often occurs during a cure reaction. This volatile material may be either a component of the original resin or a

product of the cure reaction such as carbon dioxide or water. The endothermic heat of vaporization and decrease in heat capacity from these volatilizations must be accounted for. In the case of high temperature decomposition reactions, the method developed by Brennan which was mentioned above can be used because the lower molecular weight volatile product can be assumed to leave the sample container immediately and thus its loss can be related to the reaction coordinate. However, resin cures take place at lower temperatures, and the release of their volatile products is often not immediate. Further, the rate of release of the volatile materials initially present in the resins will increase with temperature and will not be related in any way to the cure reaction which is being investigated. We discuss solutions to these problems of accounting for mass loss later.

Another problem in the analysis of cure reactions is that the glass transition temperature increases with increasing degree of cure. Cure reactions take place extremely slowly in the glassy state, so resin cures performed under isothermal conditions effectively cease when the glass transition temperature reaches the isothermal reaction temperature and the total realizable amount of cure is a function of the reaction temperature. Cure reactions performed at constant heating rate are either driven to as complete a conversion as is obtainable, or if the “ceiling” temperature is exceeded, the reverse depolymerization reaction becomes dominant. Thus, for a constant heating rate, the “initial” glass transition temperature of the resin in a cure experiment is sometimes near the initial (room) temperature and the “final” glass transition temperature of the cured polymer is often at the “final” temperature. This shifting glass transition temperature leads to problems when one attempts to assign a dynamic baseline to the cure peak in order to determine the fractional conversion.

Much of the above problems and ambiguities can be avoided by integration of DSC traces. Integration presents a simpler and clearer picture, and corrections become automatic. Such integration techniques have been applied effectively to resin cure reactions by Chang [17] and Richardson [18]. The schematic representation of integral DSC traces of  $\Delta H$  vs.  $T$  for a typical exothermic resin cure at constant heating rate is shown in Fig. 9. The curves are for DSC curves integrated over the isothermal baselines. In these cases there has been no change in mass ( $\Delta C_p$ ) during the DSC scans. Curve (I) in Fig. 9 is for a DSC run on the neat resin without catalyst so that no cure took place during the scan. Curve (II) in Fig. 9 represents the cure reaction (with catalyst added) and curve (III) is a final DSC run on the cured epoxy product from case (II). The glass transition temperature of the neat resin is represented by  $T_g(\text{resin})$  and the glass temperature of the cured epoxy by  $T_g(\text{epoxy})$ . The glass curves have been extrapolated to higher temperatures and the (supercooled) liquid curves to lower temperatures.

It is obvious that in order to determine the enthalpy and fractional

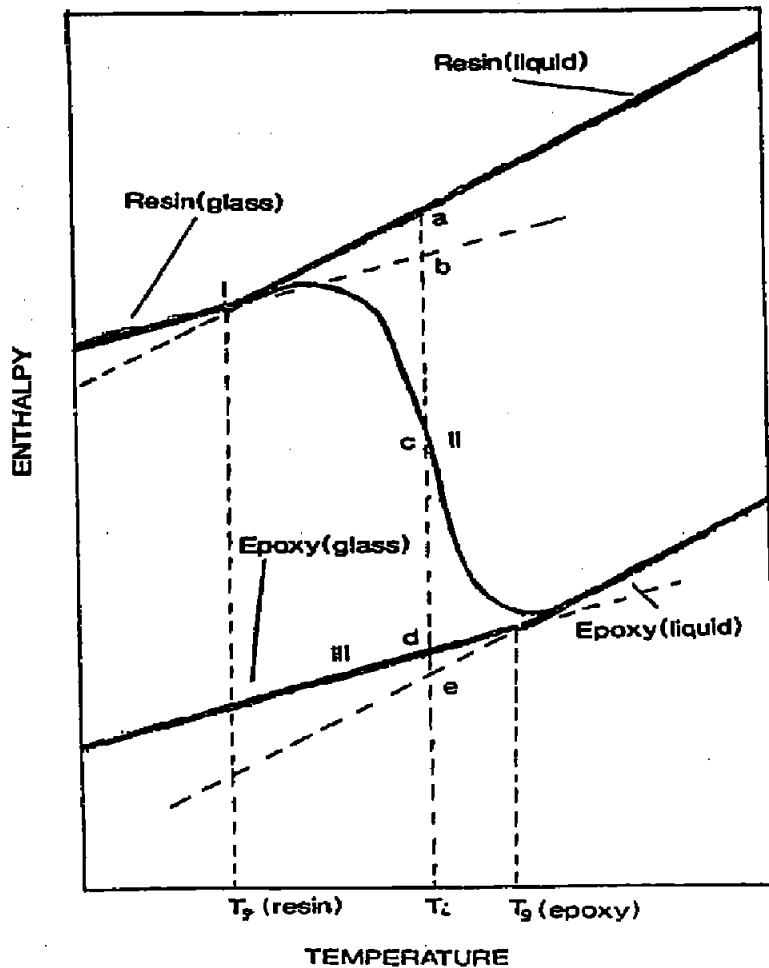
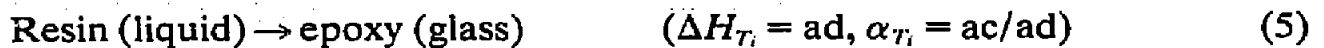
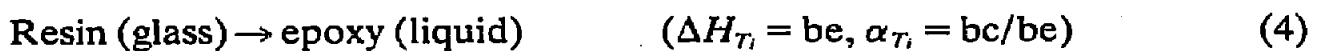


Fig. 9. Typical integral plots of  $\Delta H$  vs. temperature for the DSC cure of a resin (no mass loss) (see Chang, ref. 17): (I) integrated DSC plot for neat resin without hardener, accelerator or catalyst (sample mass "normalized"); (II) integrated DSC plot for the cure reaction; (III) integrated DSC plot for the cured epoxy.

conversion  $\alpha$  at any temperature  $T_i$  one must first define the reaction. In this case the four possible reactions which one may consider are

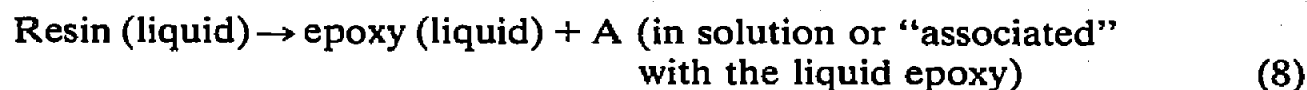
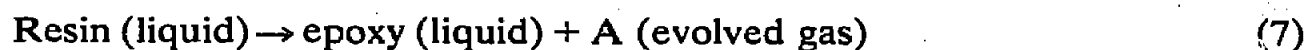


Thus we may obtain different reaction enthalpies (and different fractional degrees of conversion) for each of the above equations, in which the physical states of the reactants and products are well defined. It is not obvious which of eqns. (3)–(6) (if any) "correctly" describe a particular cure reaction, but they are all valid equations. Perhaps eqn. (6) gives the



most useful value for the enthalpy of cure because these reactions must take place in the liquid state rather than in the glassy state (where their rates are orders of magnitude slower). The equation to apply to the calculation of the fraction reacted is even less obvious. The physical structure is rather ambiguous during the cure reaction because gels and other complex structures may form. Thus the state of the system is poorly defined and so also must be the fractional conversion  $\alpha$ , which depends upon initial and final values of the enthalpy. As in the case of the enthalpy, use of the liquid  $\rightarrow$  liquid equation (eqn. (6)) would tend to be favored, for the same reason as above—the cure reactions do not occur in the glassy state.

When there is mass loss during the reaction, the stoichiometric equation must, of course, reflect this fact. For example, two extreme cases when there is a product A other than the epoxy are



The difference between the enthalpies calculated for eqns. (7) and (8) will be, of course, the latent heat of vaporization of product A as reflected by the change in  $C_p$  (heat capacity integral). When the evolved gas is part of the stoichiometry, as in eqn. (7), then a "correct"  $\Delta H_T$  can be obtained by extrapolating the integrated liquid curve back from a high temperature region where the gas A has been completely driven off.

If volatiles are present initially in the reactants and/or if the evolution of products is slow at the reaction temperature, some method of relating this weight loss to time (and temperature at constant heating rate) is needed for construction of a "running" baseline if one is to be able to calculate the fraction reacted from the enthalpy up to point  $T_i$  divided by the total enthalpy of reaction. Such a relationship can be obtained from a simultaneous DSC–TGA instrument. If both enthalpy and weight change data are available, then the Kirchhoff ( $\Delta C_p$  integral) correction for the enthalpy can be calculated as a function of time (temperature) from the fractional weight loss vs. temperature data obtained from the TGA measurement.

Sealed pressurized sample pans are often used to contain any volatile materials. There is no mass loss in such a case, so eqn. (8) would appear to be applicable. However, there is another complicating factor which must be kept in mind here. The mass loss problem is avoided but the DSC is no longer measuring  $\Delta C_p$  (at constant pressure) from which  $\Delta H$  is calculated by integration. In this case, one is measuring  $\Delta C_v$  (at constant volume) and calculating  $\Delta E$  by integration (so that  $PV$  data are needed to convert to  $\Delta H$ ).

Furthermore, it is also quite obvious that, if the entrapped vapors in the

sealed containers are the product of the chemical reaction of interest or if a measured physical transformation involves a pressure increase, then, from Le Chatelier's Principle, the chemical or physical equilibrium will be forced in the direction of the condensed phase when sealed sample containers are used.

#### IMPURITY DETERMINATION BY DSC

DSC is used to determine fractions of impurities in compounds by measuring their "freezing point depression or solubility curves". (In order to avoid problems such as "glassing" or decomposition, these experiments are usually performed at increasing rather than decreasing rates of temperature change so that "melting point depression" curves are obtained). The method is based upon the application of van't Hoff's [19] modification of the Clapeyron–Clausius equation for dilute solutions (eqn. (9)) to the DSC melting peak of a substance

$$-d \ln x_1 = -d \ln(1 - x_2) = -(\Delta H_f/R) d(1/T) \quad (9)$$

where  $x_1$  is the mole fraction of the major component (the substance whose purity is being measured),  $x_2$  is the mole fraction of the minor component (impurity) in the liquid phase,  $R$  is the gas constant, and  $\Delta H_f$  is the molar heat of fusion of the pure substance. The development of the theory behind this method and its application to impurity measurement has been presented in a thorough and precise manner by Wunderlich [20].

There are two conditions which must be met before eqn. (9) is applicable to impurity determination: (a) the compound and its impurity(ies) must form a single liquid solution; (b) the compound and its impurity(ies) must not form a solid solution, i.e. they must exist in separate phases in the solid (and, therefore, their phase diagram must have a eutectic).

Equation (9) may be integrated between  $T_i$  and  $T_j$ , any two temperatures between the eutectic temperature and the final melting temperature of the major component in equilibrium with the liquid solution of the components, to obtain

$$\ln(1 - x_2)_i - \ln(1 - x_2)_j = (\Delta H_f/R)(1/T_i - 1/T_j) = \Delta H_f(T_j - T_i)/RT_iT_j \quad (10)$$

taking  $\Delta H_f$  as constant over the temperature range  $T_i$ – $T_j$ .  $\Delta H_f$  is obtained from the integration of the area under the total DSC melting peak.

The common method for purity determination makes use of a continuous DSC scan at constant heating rate (see, for example, the first seven papers of ref. 21). It utilizes two mathematical approximations of eqn. (10). First  $(1/T_i - 1/T_0) = (T_0 - T_i)/T_0T_i$  is put equal to  $(T_0 - T_i)/T_0^2$  (which is satisfactory at ambient or above ambient temperatures). Secondly,  $\ln(1 - x_2)$  is set

equal to  $x_2$  (the first term of its series expansion, which is satisfactory for small  $x_2$ ; the error from using this approximation is 1.0% for  $x_2 = 0.02$  and 2.6% for  $x_2 = 0.05$ ). Including these approximations into eqn. (10), one obtains

$$T_0 - T_i = (RT_0^2 x_2) / (\Delta H_i F_i) \quad (11)$$

where  $F_i$  is the fraction of sample molten at  $T_i$ .  $F_i (= \Delta H_i / \Delta H_f)$  is obtained from areas under the DSC melting peak(s) where  $\Delta H_i$  is obtained from the partial area melted at  $T_i$ .  $T_0$  is obtained from the extrapolation of  $1/F_i$  vs.  $T_i$ , which from eqn. (11) should give a straight line with intercepts  $T_0$  at  $1/F_i = 0$  and  $T_m$  (the temperature at the last trace of melting) at  $1/F_i = 1$ .

However, owing to the fact that thermodynamic equilibrium is never even closely reached during the continuous heating rate method, a purely arbitrary "linearization correction" (typically 5–10% of  $F$ ) is necessary to obtain a straight line for the  $1/F_i$  vs.  $T_i$  plot [21]. Further, if the amount of impurity is small, the eutectic is not detected by this continuous scan technique, so the possibility of a solid solution is not eliminated.

Therefore, a method in which the temperature is increased in stepwise increments (see, for example, refs. 22–25) is to be preferred because the specimen is allowed to approach thermodynamic equilibrium between each step and the eutectic, even when the amount of impurity is small, can usually be detected. (The eutectic will manifest itself by a larger peak at the temperature step at the beginning of the stepwise temperature scan through the melting range: see, for example, Fig. 1 of ref. 23.) (The presence of a eutectic does not preclude the possibility of an undetected second impurity which forms a solid solution with the major component.)

However, here we review a two (or more) step method developed by Wunderlich [20] from the work of Gray and Fyans [22]. The experimental procedure is essentially the same as that described in a previous section on isothermal temperature calibration. However, for this case where an enthalpy change is to be determined, one must subtract from it the enthalpy change due to the difference in heat capacities between the sample side (including the specimen) and the reference side. This correction can be determined from integration of the areas for temperature steps, either just before or just beyond the transition (during which no enthalpic event are occurring). Once these areas have been determined for (preferably large) temperature steps in the range of interest, the heat capacity enthalpy correction per degree can be calculated so that an appropriate blank can be subtracted from the enthalpy determined for each temperature step during the melting transition.

In this method, incremental heats of fusion  $\Delta H_1, \Delta H_2, \dots, \Delta H_i$  are measured for successive and evenly spaced temperature steps  $T_1, T_2, \dots, T_i$ , where the system is allowed to thermodynamically equilibrate after each step. If  $\Delta H_a$  is the unmeasured heat of fusion up to a starting

temperature  $T_n$ , then the fraction molten is given by

$$F_n = \left( \Delta H_a + \sum^n \Delta H_n \right) / \Delta H_f \quad (12)$$

and eqn. (11) for the  $n$ th melting step becomes

$$T_n = T_0 - RT_0^2 x_2 / \left( \Delta H_a + \sum^n \Delta H_n \right) \quad (13)$$

$\Delta H_a$  can be eliminated from eqn. (13) for two successive steps to obtain

$$\Delta H_n = RT_0^2 x_2 \Delta T / [(T_0 - T_n)(T_0 - T_n + \Delta T)] \quad (14)$$

where  $\Delta T = T_n - T_{n-1}$  is the constant temperature difference between any two successive steps.  $RT_0^2 x_2$  can be eliminated by forming the ratio

$$\Delta H_n / \Delta H_{n-1} = 1 + 2\Delta T / (T_0 - T_n) \quad (15)$$

and, finally, the mole fraction of impurity  $x_2$  can be calculated by substituting  $T_0$  from eqn. (15) into eqn. (14) to obtain

$$x_2 = 2\Delta H_n (2 + B) / R\Delta T [(BT_n / \Delta T) + 2]^2 \quad (16)$$

where  $B = (\Delta H_n / \Delta H_{n-1}) - 1$ . Thus the mole fraction of impurity  $x_2$  is determined directly from two successive partial heats of fusion which are calculated for two successive temperature steps  $(T_n - T_{n-1}) = \Delta T$  [20]. The two successive temperature steps should be separated widely enough to result in reasonably large values for  $\Delta H_n$  and  $\Delta H_{n-1}$  for greatest accuracy, but not too near the beginning nor at the end of the melting temperature range.

## CONCLUSIONS

The integration of DSC curves between two isothermal temperatures avoids many of the problems present in the analysis of "differential" dynamic DSC curves when they are used to calibrate temperature and enthalpy and to calculate heat capacity and impurity content. Correct thermodynamic properties are obtained through interpretation of the integrated curves. The integrated curves are superior for the visual comprehension of enthalpy changes during glass and first order transitions, and for the calculation of proper glass transition temperatures, heat capacity changes, heats and temperatures of transition or reaction, and fractions reacted.

## REFERENCES

1. A.L. Lavoisier and P.S. Laplace. *Oeuvres*, tome ii, 1783, p. 283.
2. T. Daniels, *Thermal Analysis*, Kogan Page, London, 1973, p. 129.
3. R.M. Flynn, J.H. Flynn and T.J. Bent, *Thermochim. Acta*, 134 (1988) 401.

- 4 J.H. Flynn, *Thermochim. Acta*, 8 (1974) 69.
- 5 Specific Heat Program, Rev. A, Perkin-Elmer, Norwalk, CT, 1977.
- 6 S.-F. Lau and B. Wunderlich, *J. Therm. Anal.*, 28 (1983) 59.
- 7 S.C. Mraw and D.F. Naas, *J. Chem. Thermodyn.*, 11 (1979) 567. S.C. Mraw and D.F. O'Rourke, *J. Chem. Thermodyn.*, 13 (1981) 199.
- 8 J.H. Flynn and D.M. Levin, *Thermochim. Acta*, 126 (1988) 93.
- 9 J.H. Flynn, in R.S. Porter and J.F. Johnson (Eds.), *Analytical Calorimetry*, Vol. 3, Plenum, New York, 1974, p. 41.
- 10 M.J. Richardson and N.G. Savill, *Polymers*, 16 (1975) 753.
- 11 J. Malik, personal communication, 1991.
- 12 A. Weitz and B. Wunderlich, *J. Polym. Sci. Polym. Phys. Ed.*, 12 (1974) 2473.
- 13 G. Adam and F.H. Muller, *Kolloid Z.Z. Polym.*, 192 (1963) 29.
- 14 C.M. Guttman and J.H. Flynn, *Anal. Chem.*, 45 (1973) 408.
- 15 G. Kirchhoff, *Poggendorf's Ann.*, 103 (1858) 185.
- 16 W.P. Brennan, B. Miller and J.C. Whitwell, *Ind. Eng. Chem. Fundam.*, 8 (1969) 314.
- 17 S.S. Chang, *J. Therm. Anal.*, (1988) 135.
- 18 M.J. Richardson, *Pure Appl. Chem.*, 64(11) (1992) 1789.
- 19 J.H. van't Hoff, *Z. Phys. Chem.*, 1 (1887) 481.
- 20 B. Wunderlich, in E. Turi (Ed.), *Thermal Characterization of Polymeric Materials*, Academic Press, New York, 1981, pp. 208–214.
- 21 R.L. Blaine and C.K. Schoff (Eds.), *Purity Determinations by Thermal Methods*, ASTM Symp. E-3/on Thermal Measurements, Baltimore, MD, 25 April 1983, ASTM, Philadelphia, PA, 1984.
- 22 A.P. Gray and R.L. Fyans, Some comments and calculations on a method of purity determination by stepwise melting, *Thermal Application Study*, Vol. 3, Perkin-Elmer, Norwalk, CT, 1972.
- 23 H. Staub and W. Perron, *Anal. Chem.*, 46 (1974) 128.
- 24 J.P. Elder, Purity analysis by dynamic and isothermal step differential scanning calorimetry, in R.L. Blaine and C.K. Schoff (Eds.), *Purity Determinations by Thermal Methods*, ASTM, Philadelphia, PA, 1984, pp. 55–60.
- 25 A.R. Ramsland, *Anal. Chem.*, 52 (1980) 1474; *Proc. N. Am. Therm. Anal. Soc. Conf.*, 23–26 September 1984, Philadelphia, PA, USA, pp. 138–144.